

Successes and failures of simplified models for a network of real neurons

Leenoy Meshulam^{1,2}, Jeffrey L. Gauthier⁸, Carlos D. Brody^{3,6,7}, David W. Tank^{3,4,6}, and William Bialek^{4,5,9}

¹*Center for Computational Neuroscience, and ²Department of Applied Mathematics,
University of Washington, Seattle, Washington 98195* ³*Princeton Neuroscience Institute,*

⁴*Joseph Henry Laboratories of Physics, ⁵Lewis-Sigler Institute for Integrative Genomics,
⁶Department of Molecular Biology, and ⁷Howard Hughes Medical Institute,
Princeton University, Princeton, NJ 08544* ⁸*Department of Biology, Swarthmore College,
Swarthmore, Pennsylvania 19081* ⁹*Initiative for the Theoretical Sciences,
The Graduate Center, City University of New York, 365 Fifth Ave., New York, NY 10016*

(Dated: December 30, 2021)

Recent breakthroughs have made it possible to acquire “big data” on a wide range of living systems, including the brain. Here we use measurements of the simultaneous activity in 1000+ neurons from the mouse hippocampus to explore the successes and failures of a class of simplified models, grounded in statistical physics. These models make quantitative, parameter-free predictions about the patterns of activity in populations of neurons, and we test a large number of these predictions against the behavior of many different groups of $N=100$ cells. When these cells are dense samples from a small region, we find extremely detailed quantitative agreement between theory and experiment, within the error bars of the experiment itself. When cells are sparse samples from larger regions, the models fail. These results suggest that success or failure for this class of models reflects underlying properties of the hippocampal network, connecting to a variety of independent experimental observations. Most importantly, these results show that we can aspire to much more than qualitative agreement between simplifying theoretical ideas and the detailed behavior of a complex biological system.

I. INTRODUCTION

The last decades have seen revolutionary changes in the quality and quantity of data that can be collected from living systems. Here we argue that recent progress in monitoring, simultaneously, the activity of more than one thousand neurons in mouse hippocampus creates a novel opportunity to test the effectiveness of a broad class of simplified models for this complex system, perhaps illustrating the question of how well models “work” more generally.

While it has long been possible, for example, to record the electrical activity of single neurons, and to trace these dynamics down to the properties of single ion channel molecules, it now is possible to monitor simultaneously the electrical activity of hundreds or even thousands of neurons, whether electrophysiologically [1–4] or optically [5–9], as animals engage in complex behaviors. In many instances the noise levels of these large scale recordings are below the noise levels of the neurons, just as in classical single neuron experiments. An example of this is seen in the raw data of Fig 1.

Capturing the full richness of these large datasets has emerged as a clear challenge, in studies of the brain and more generally. There has been considerable emphasis placed on the quantity of data in these experiments, but here we emphasize that the increasing quality of data should elevate our expectations for the comparison of theory and experiment. In measurements on single ion channels, for example, we expect that a description of the underlying dynamics in terms of states and voltage-dependent transitions of the protein will agree with experiment within the measurement errors; disagreement

between theory and experiment is a sign that we are missing some feature of these molecular dynamics. It would be satisfying if we could hold our theories of neural populations to a similarly stringent standard.

In one view, the increasing number of dynamical variables that is being monitored means that we need much larger models. This exploration of very large models has a long history, including, for example, the search for complete models of cellular metabolism [10]. The enormous success of deep neural networks has given considerable impetus to the study of very complex models, showing that we can have effective predictions even when data are far from sufficient to determine all the underlying parameters [11–13].

The alternative view is that as systems become more complex it becomes even more important to search, explicitly, for simplification. An example is the idea that the dynamics of activity in a network of N neurons might be confined to a d -dimensional space, with $d \ll N$ [14–17]. A different kind of simplification is suggested by statistical physics, where successful models for macroscopic behaviors of materials often are much simpler than the underlying microscopic mechanisms [18]. One systematic implementation of this idea is the maximum entropy method, where we match some features of the data but otherwise the model has as little structure as possible [19, 20]. Maximum entropy models are mathematically equivalent to problems in statistical physics, giving us access to a range of analytic and numerical techniques. The connection to statistical physics also implies that at large N these models typically have distinct phases with qualitatively different behaviors, as with gases, liquids, and solids. If the maximum entropy models provide accurate descriptions of real neural networks, it becomes sensible

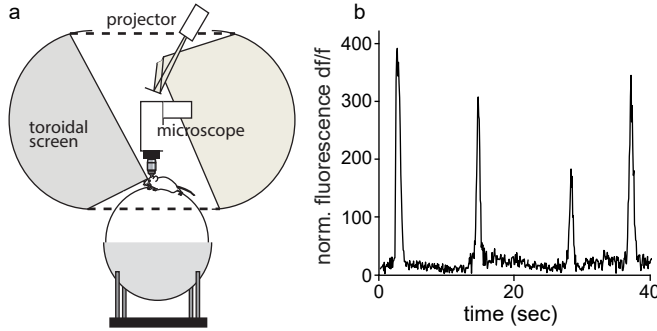


FIG. 1: Experimental setup. (a) Schematic showing the virtual reality setup where a two-photon microscope is used to image large-scale neuronal populations in a head-fixed mouse. The feedback from the animal running on the ball advances the virtual corridor projected on the spherical screen. (b) An example trace of fluorescence level from a CA1 neuron, showing the high SNR typical to experiments of this kind. Raw data was motion corrected and normalized.

to ask where these networks sit in the phase diagram of possible networks.

Maximum entropy methods have been used to describe the collective behavior of neural populations [21–27], the variation of amino acid sequences in protein families [28–31], the antibody repertoire in the immune system [32, 33], and the ordering of flight velocities in flocks of birds [34, 35]. Despite important successes, there are reasons to be skeptical. Some authors have gone so far as to claim that maximum entropy models can describe patterns of neural activity only in uninteresting limits of weak correlation [36, 37]. At the opposite extreme we might worry that these models are just complex enough to describe a very wide range of behaviors, so that “success” is almost guaranteed and doesn’t teach us anything about the brain.¹

Recent progress on measurements and models for neural activity in the mouse brain creates a novel opportunity to test the effectiveness of the maximum entropy approach, perhaps illustrating the question of how well models “work” more generally. Experiments using calcium imaging during exploration in virtual environments have advanced from monitoring tens to hundreds to thousands of neurons simultaneously [16, 39–41]. We have found that the distribution of activity across populations of ~ 100 cells in dorsal hippocampus can be described very accurately by maximum entropy models [42], yet for the reasons outlined above it is not clear whether the

degree of accuracy that we observe is significant. But recording from thousands of neurons offers the opportunity to choose groups of 100 cells in many different ways.

We exploit 1000+ neuron recordings to choose many different sub-populations of $N = 100$ neurons, and then construct individual maximum entropy models for each of these groups. We find that when the group of cells is spatially contiguous (“local” subgroups), maximum entropy models that match pairwise correlations predict a wide range of higher order structure in the patterns of neural activity. But if we draw the same number of cells at random from a larger area (“distant” subgroups), the agreement deteriorates. These results are aligned with previously reported observations in the literature that neural activity in dorsal hippocampus is spatially organized [43–45]. Importantly, in the most successful examples all of the higher order statistical features of network activity that we test are predicted, within experimental error, by the maximum entropy distribution. This sets a high standard for what we mean when we say that a model works.

II. STRATEGY

Imaging large neuronal populations

The experiments analyzed here monitor, simultaneously, activity of more than 1000 neurons in the CA1 region of the mouse hippocampus. Briefly, mice have been genetically engineered to express GCaMP3, a calcium-sensitive fluorescent protein, and the resulting fluorescence is imaged simultaneously for many neurons using a scanning two-photon microscope. The mouse runs on a floating ball while its head is fixed, and the rotation of ball is fed back to a visual stimulus to create the virtual experience of running along a 4 m track. Figure 2a shows a field of view of the dataset we focus on in the body of the paper, which consists of a $N_{\text{total}} = 1485$ neurons in a $433 \times 433 \mu\text{m}^2$ area; each pixel in the image is $0.87 \times 0.87 \mu\text{m}^2$. For each identified cell we compute its pixels’ center of mass, and those are indicated in Fig 2b. Experimental details, including the algorithms for reducing images to traces of activity in individual neurons, can be found in Refs [41, 46].

The hippocampus plays a critical role in episodic memory by forming patterns of activity that represent specific memories. A prominent example of such memories are spatial locations, encoded by “place cells” that are active only when the animal visits a particular location in the environment [47–49]. A collection of place cells often is referred to as a “cognitive map,” and is thought to contribute to the animal’s navigation ability in space. In the CA1 region of the hippocampus 30% – 50% of neurons are thought to be place cells in any single experimental environment [41, 42, 49].

The output of each imaging experiment is a $T \sim 40$ min long time series with frames of duration $\Delta\tau = 1/30$ s

¹ The class of maximum entropy models discussed here is equivalent to Ising models with competing interactions. Since the decision form of Ising spin glasses is NP-complete [38], a broad class of computational problems can be mapped to asking about the ground state of a spin glass. In this sense, the Ising models we consider below describe almost arbitrarily complex systems, albeit through some possibly complex transformation.

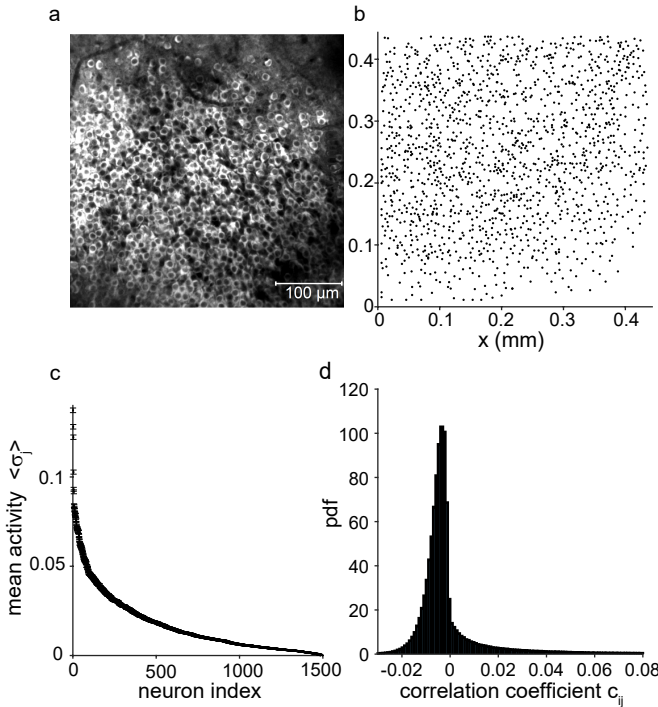


FIG. 2: Neural activity in a large population of CA1 hippocampal neurons. (a) Fluorescence image of 1485 neurons expressing calcium-sensitive fluorescent protein (averaged). Field of view $433 \times 433 \mu\text{m}^2$. (b) Centers of mass locations for all neurons found in the field of view shown in (a). (c) Mean activity of the discrete, binarized activity for all neurons in (a), in descending order. (d) Probability distribution of correlation coefficients, c_{ij} , as defined in Eq (2), across all pairs of neurons in (a).

for each of the 1000+ neurons. Each series includes all time points of the session—not only concatenated running times, but also all inter-trial intervals when the mouse paused to receive a drop of water as a reward. After denoising the fluorescence signal, we binarize each neuron’s activity value in each frame, based on whether it was active or silent, $\sigma_i \in \{0, 1\}$; details can be found in Ref [42]. We note that deconvolving and discretizing fluorescent signals is an involved topic with much research supporting different methods [50–52]. However, for the purpose of this study, and given that neurons in CA1 tend to fire strongly and more than one spike at a time (“bursts”), the simple on/off approach is satisfactory. In our hands, applying more sophisticated methods for this process did not alter any of the results described here. Figures 2c and d summarize basic features of these data, showing that individual neurons are active less than 10% of the time and that pairs of neurons are weakly correlated.

Assembling subgroups

We would like to exploit the recordings from 1000+ neurons to analyze many different subgroups of $N = 100$ cells. To begin we can choose a cell at random and draw a circle of radius $r = 0.07 \text{ mm}$. This circle contains roughly one hundred cells, and simulates the previous generation of experiments in which we had a more limited field of view [42]. We will refer to the cells from this small radius as a “local” subgroup of neurons.

With the same cell at the center, we can draw circles of progressively larger radii— $r \sim 0.11, 0.14, 0.18, 0.22 \text{ mm}$, increasing by a factor of two in area at each step—and then draw cells at random from these larger regions. But for the different groups to be comparable we want to keep the fraction of place cells fixed; this turns out to keep the distribution of mean activities $\langle \sigma_i \rangle$ across the group roughly constant as well. Because the models we study (see below) are built by matching the correlations between pairs of cells, we would also like to fix the distribution of these correlations. Concretely, as move from one radius (r_k) to the next (r_{k+1}) we keep track of the covariance matrix elements,

$$C_{ij} = \langle (\sigma_i - \langle \sigma_i \rangle)(\sigma_j - \langle \sigma_j \rangle) \rangle. \quad (1)$$

In any given group we can form the distribution of these matrix elements, $P_k(C)$ in the group at radius r_k . To move from $r_k \rightarrow r_{k+1}$ we swap cells in the smaller radius for those in the larger radius, and at every swap we minimize the Kullback–Leibler divergence between $P_k(C)$ and $P_{k+1}(C)$, until half of the cells have been swapped.² The result of this process is a nested collection of groups drawn from progressively larger regions of the same brain area and matched in their basic statistical properties; Fig 3 shows an example of the smallest (“local”) and largest (“distant”) groups.

Note that because we swap half the cells as we increase the area of the sampling region by a factor of two, the distribution of cells in the different groups stays uniform with decreasing density. One could also think of these subgroups as simulating an experiment where we sample at random from only a fraction of the cells in a region, down to $\sim 10\%$ at $r = 0.22 \text{ mm}$. We also note that while we explicitly constrain the distribution of covariance matrix elements (as seen in Fig 3c-d), the distribution of the correlation coefficients

$$c_{ij} = \frac{C_{ij}}{\sqrt{C_{ii}C_{jj}}}, \quad (2)$$

also remains very nearly fixed (Fig 3e-f).

² Forming these distributions from the $N(N - 1)/2$ pairs requires binning or interpolating along the C axis. To make comparisons as straightforward as possible, we used a fixed set of 300 bins at all r .

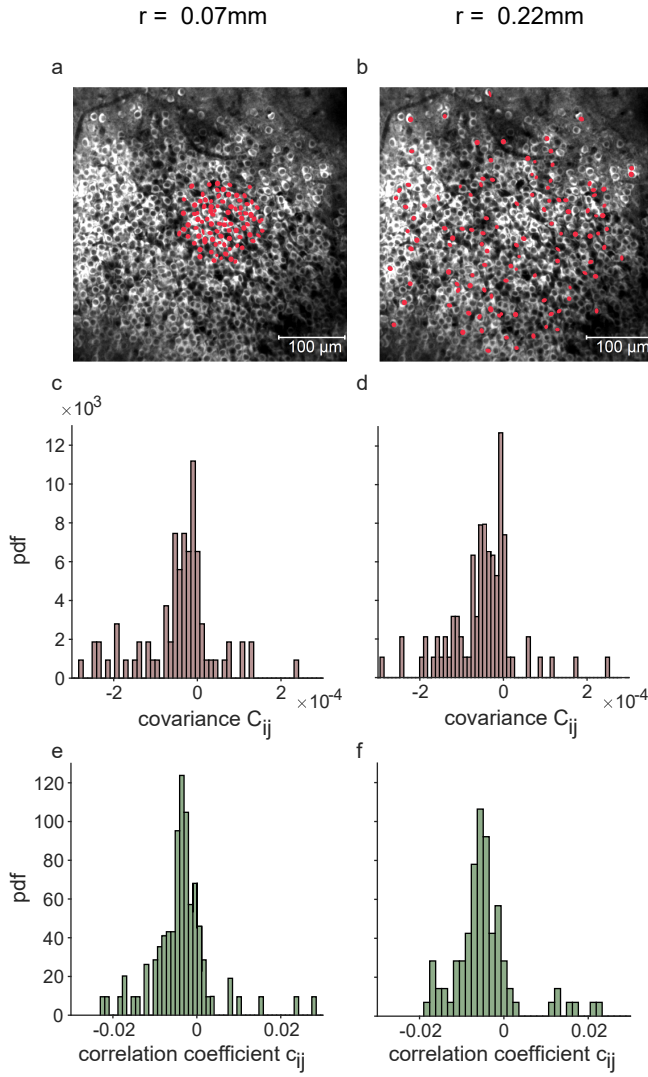


FIG. 3: Constructing “local” and “distant” subgroups. (a) Fluorescence image of the entire field of view, as in Fig 2a. Red marks overlaid depict the cells included in an example local subgroup. (b) Fluorescence image of the entire field of view, as in Fig 2a. Red marks overlaid depict the cells included in an example distant subgroup. (c) Probability distribution of covariances, as defined in Eq. 1, for the local neurons indicated in red in panel a. (d) Probability distribution of covariances, as defined in Eq. 1, for the distant neurons indicated in red in panel b. (e) Probability distribution of correlation coefficients, as defined in Eq. 2, for the local neurons indicated in red in panel a. (f) Probability distribution of correlation coefficients, as defined in Eq. 2, for the distant neurons indicated in red in panel b.

Maximum entropy models for subgroups

In each of the subgroups we are faced with a population of $N = 100$ neurons, and in each small window of time ($\Delta\tau = 33$ ms) every cell either is active ($\sigma_i = 1$) or silent ($\sigma_i = 0$). The state of the entire network then is an N -bit

binary vector $\{\sigma_i\} = \{\sigma_1, \sigma_2, \dots, \sigma_N\}$. A theory of the network should be able to predict the probability that we find the system in any one of these states, $P(\{\sigma_i\})$, essentially telling us how surprised we should be by any pattern of activity and silence in the network.

The maximum entropy method is a strategy for constructing approximations to the distribution $P(\{\sigma_i\})$ [19, 20]. This method now has been used quite widely in analyzing networks of neurons [21–27] and other examples of collective behavior in living systems [28–35], but to make our presentation self-contained we review some basic notions here.

The essential idea is to explore models $P(\{\sigma_i\})$ that have as little structure as possible, or equivalently generate network states $P(\{\sigma_i\})$ that are as random as possible, while still matching some observed properties of the system. It is a theorem that the only way to turn “as random as possible” into something mathematically precise is to maximize the entropy of the distribution $P(\{\sigma_i\})$ [53],

$$S = - \sum_{\{\sigma_i\}} P(\{\sigma_i\}) \log [P(\{\sigma_i\})]. \quad (3)$$

There is no unique choice for which properties of the system we should match.³ For a network of neurons, it makes sense that our model should at least match the mean activity of every neuron, so we insist that for each cell j we have

$$\langle \sigma_j \rangle \equiv \sum_{\{\sigma_i\}} P(\{\sigma_i\}) \sigma_j = \langle \sigma_j \rangle_{\text{expt}}, \quad (4)$$

where $\langle \dots \rangle_{\text{expt}}$ is the average across the experiment. As a first step toward capturing the interactions among neurons in the network, we can also match the correlations between the activity in all pairs of cells, as measured by the covariance [Eq (2)] or correlation coefficient [Eq (1)] (shown in Fig 2d for all pairs of cells). Given that we have constrained the means in Eq (4), this is equivalent to insisting that for each pair jk ,

$$\langle \sigma_j \sigma_k \rangle \equiv \sum_{\{\sigma_i\}} P(\{\sigma_i\}) \sigma_j \sigma_k = \langle \sigma_j \sigma_k \rangle_{\text{expt}}. \quad (5)$$

The probability distribution that maximizes the entropy in Eq (3) while obeying the constraints in Eqs (4)

³ To be clear, this means that there is no such thing as “the” maximum entropy model. There are many possible maximum entropy models, depending on our choice of what to match.

and (5) has the form

$$P(\{\sigma_i\}) = \frac{1}{Z} \exp[-E(\{\sigma_i\})] \quad (6)$$

$$E(\{\sigma_i\}) = - \sum_{i=1}^N h_i \sigma_i - \frac{1}{2} \sum_{i,j=1}^N J_{ij} \sigma_i \sigma_j. \quad (7)$$

$$Z = \sum_{\{\sigma_i\}} \exp[-E(\{\sigma_i\})]. \quad (8)$$

To complete the construction we actually have to find the parameters $\{h_i, J_{ij}\}$ that solve Eqs (4) and (5). This model is equivalent to the statistical mechanics problem of Ising spins in magnetic fields h_i and interacting through couplings J_{ij} [54]. We use Monte Carlo simulation to draw large numbers of samples out of the distribution in Eqs (6–8), compute the expectation values $\langle \sigma_j \rangle$ and $\langle \sigma_j \sigma_k \rangle$, and adjust the parameters $\{h_i, J_{ij}\}$ until Eqs (4) and (5) are satisfied, as in Ref [42].

A crucial feature of the maximum entropy method is that once we have matched the measured mean activities and pairwise correlations among cells, there are no free parameters. Thus we can make *parameter-free* predictions for all the higher order statistical structure in the network. Indeed one could view this approach not as a proposing a class of models for the system but as an engine for connecting different aspects of the data. With small numbers of neurons we could make these connections explicit, e.g. writing the correlations among three neurons as a function of the mean activities and pairwise correlations, with no adjustable parameters. At large N this becomes impossible and we rely on Monte Carlo simulations of the model as an intermediary. The essential simplification that makes possible all these predictions is the hypothesis that all relevant structure is encoded in the pairwise correlations, and of course this needs to be tested.

Scope

For each of three different datasets, in three different mice, we have chosen ten different neurons as the center for the assembly process described above, and then built maximum entropy models for the “local” ($r = 0.07$ mm) and “distant” ($r = 0.22$ mm) subgroups of $N = 100$ cells. As detailed below, each of these sixty models is subjected to six different tests. We focus on the comparison of local vs distant populations in one typical dataset. We also have constructed models for populations at intermediate radii, to see how the quality of predictions varies systematically with the size of the region, and these results will be discussed in a longer paper.

III. RESULTS

The pairwise maximum entropy models match the first and second moments of neural activity, by construction,

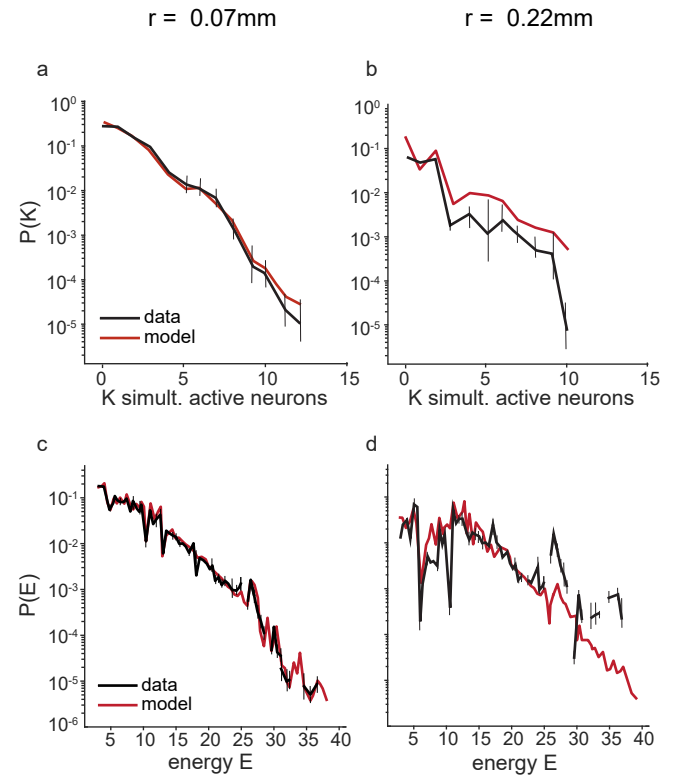


FIG. 4: **Multi-neuron simultaneous activity and the probability distribution of effective energies.** (a) The probability that K out of the $N = 100$ neurons in the subgroup population are active simultaneously, for the “local” subgroup. Model predictions depicted in red, data in black. Values for the data depict mean and standard deviations over random halves of the experiment. (b) Same as panel a, computed for the “distant” subgroup. (c) The distribution of effective energies, $P(E)$, or log probabilities, that the model assigns to every possible state in the network, computed for the “local” subgroup. In black, the distribution over population states as observed in the experiment. In red, the distribution predicted from the model. Values for the data depict mean and standard deviations over random halves of the experiment. (d) Same as panel c, computed for the “distant” subgroup.

and then make parameter-free predictions for all higher order structure in the patterns of activity across the population. We have examples where these predictions have been successful [26, 27, 42], but this success is not at all guaranteed [55, 56], especially at the scales that we consider here. In this section we look systematically at six different predictions, contrasting the levels of success that we find for local and distant subgroups.

Simultaneous activity

The maximum entropy model aims to capture the *collective* nature of population activity. A first test of these predictions is to ask for the probability that K out of the

N neurons are active in the same small window of time, $P(K)$. Figure 4a shows this distribution for the “local” subgroup, and Fig 4b shows the same distribution for the “distant” one. We note the significant difference in quality of agreement between theory and experiment in these two cases: the local subgroup predictions stay within experimental error bars throughout the entire range, even down to probabilities $10^{-4} - 10^{-5}$ at $K > 10$. In contrast, the distant subgroup predictions are out of measurement error bounds for all $K > 3$. It seems worth noting that if we only saw Fig 4b we might be tempted to conclude that agreement with experiment is not bad; after all this is a complex biological system and we have written a simple physics-style model. Figure 4a demonstrates that truly quantitative agreement, within error bars, is possible, using the same class of models for neurons in the same region of the brain. We find this consistently in all of the twenty local subgroups that we constructed, as will be described fully in a longer paper.

Log probabilities of states

The maximum entropy approach predicts the probability of all possible combinations of activity and silence in the network, $P(\{\sigma_i\})$. The fundamental quantity in this prediction is the “energy” or log probability $E(\{\sigma_i\})$ from Eq (7), which we can compute for every network state. This means that we can look at the distribution of energies across the experimentally observed states, as well as the distribution that is predicted from the theory itself. The mapping to statistical physics problems tells us that this distribution is an important test of the details of our description [57]. Figures 4c and d show these distributions, $P(E)$, for theory and experiment in both local and distant subgroups. Predictions are in excellent quantitative agreement with experiment for the spatially contiguous or local subgroup (Fig 4c), including small detailed structures that one might be tempted to dismiss as noise but in fact are significant. Agreement extends to $E > 30$, corresponding to individual network states with relative probabilities of $\sim 10^{-13}$. There is no way that we could verify the probabilities of these individual states, but these results show that the distribution of these energies over all states is predicted correctly. In contrast, predictions in the distant subgroup depart from experimental data already at $E \sim 7$ (Fig 4d).

Triplet correlations, in groups

We have constructed maximum entropy models that match correlations in the activity of pairs of neurons. In some sense the most natural test of the theory then is to ask if we can predict correlations or covariance in the activity of triplets,

$$C_{ijk} \equiv \langle (\sigma_i - \langle \sigma_i \rangle)(\sigma_j - \langle \sigma_j \rangle)(\sigma_k - \langle \sigma_k \rangle) \rangle \quad (9)$$

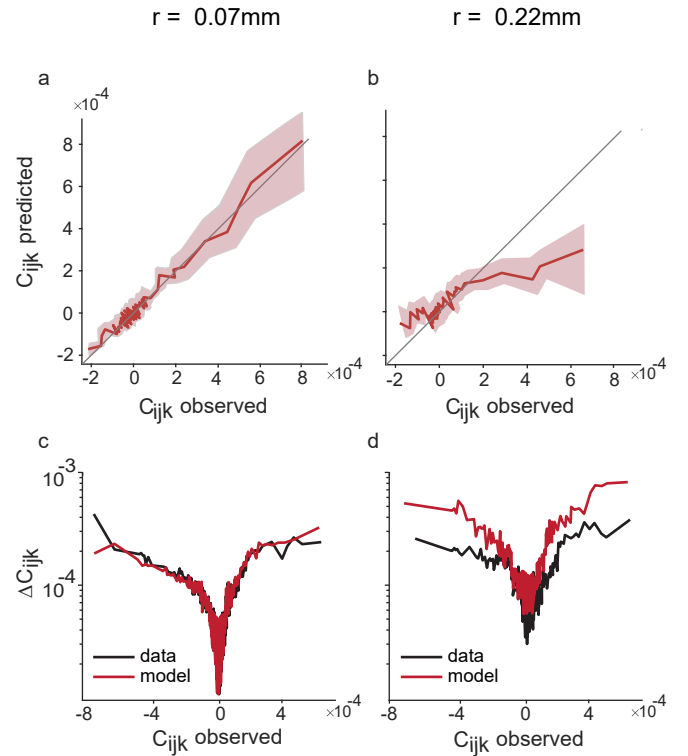


FIG. 5: **Triplet correlations.** (a) Comparison of the maximum entropy model prediction errors for individual triplet correlations, C_{ijk} as defined in Eq (9), and the measurements errors computed from the data itself for the “local” subgroup. (b) Same as panel a, computed for the “distant” subgroup. (c) Binned values of triplet correlations computed for the subgroup of neurons of the “local” subgroup. On the x-axis, the $\sim 1.6 \times 10^5$ values of individual triplet correlations are grouped together into adaptive bins. The corresponding values computed from the model are binned in the same way, shown on the y-axis. Shaded area indicated standard deviation of prediction across bins. (d) Same as panel c, computed for the “distant” subgroup.

For a populations of $N = 100$ cells, there are $\sim 1.6 \times 10^5$ distinct ways to choose a triplet. In Fig 5a-b we group the measured triplet correlations into bins, and show the mean and standard deviation in each bin. To compare, we plot those values computed from the model and from the data against each other. Here again the accuracy of model predictions reflects the subgroup’s spatial scale. For the local subgroup, predictions are within experimental error across the full dynamic range of the data (Fig 5a). For the distant subgroup, in contrast, there is quite a dramatic mismatch between theory and experiment, with limited success only at the smallest triplet correlation values (Fig 5b).

Triplet correlations, individually

For a different perspective on our model's performance predicting correlations among triplets of neurons, we consider a less forgiving test: instead of grouping correlation values together and comparing means, we scrutinize the level of theory/experiment agreement for each of the $\sim 1.6 \times 10^5$ triplets individually. Concretely, we compute the mean square difference between each predicted and measured correlation (inside small bins) as well as the mean square error in our measurements. In each one of the panels of Fig 5c-d, we show the square root of these two values, effectively the errors in measurement (black) and predictions (red). Without overfitting, it is hard to perform any better than the model does in the case of the local subgroup (Fig 5c). However, the model of the distant subgroup exhibits poorer performance. Not only does it have a much higher error than empirically measured for the extreme values in the range, its error values also systematically exceed the experimental ones at small C_{ijk} , which are the values observed most frequently (Fig 5d).

What the population tells us about one neuron

One of the characteristics of a population whose behavior is collective is that the population-level activity can be strongly predictive of individual member's activity. We leverage the equivalence between our maximum entropy model and an Ising model with competing interactions, and borrow the concept of an "effective field," h_i^{eff} . This quantity is a measure of how a full population of cells influences one neuron among it, and is defined as:

$$h_i^{\text{eff}} = E(\sigma_1, \dots, \sigma_i = 0, \dots, \sigma_N) - E(\sigma_1, \dots, \sigma_i = 1, \dots, \sigma_N) \quad (10)$$

$$= h_i + \sum_{j \neq i} J_{ij} \sigma_j. \quad (11)$$

We can use the effective field to predict the probability that any single neuron is active, at any moment in time, given the active/silent state of all the other neurons in the population at the same moment,

$$q \equiv P(\sigma_i = 1 | h_i^{\text{eff}}) = \frac{1}{1 + \exp(-h_i^{\text{eff}})}. \quad (12)$$

In Fig 6a-b we test these predictions: we obtain an effective field value for each neuron at every moment in time, which is dependent on the active/silent state of the rest of the population, and then pool all of these values together. Each of the panels depicts the probability of a neuron to be active against the effective field of the same neuron, on top of the logit function [Eq (12)]. While the agreement between theory and observations is very good for the local subgroup (Fig 6a), even for very large effective fields, prediction quality drops significantly for the distant subgroup (Fig 6b).

What one neuron tells us about the population

To further investigate the relationship between an individual cell's activity and the state of the rest of the population, we ask a complementary question: Does a neuron being active (silent) predict a high (low) value of the effective field? This is related to the comparisons in Fig 6a,b via Bayes rule:

$$P(h_i^{\text{eff}} | \sigma_i = 1) = \frac{P(\sigma_i = 1 | h_i^{\text{eff}}) P(h_i^{\text{eff}})}{P(\sigma_i = 1)}. \quad (13)$$

There is no "correct" distribution of h_{eff} , but it would be attractive if neurons being active predicted that the whole network is in a state that favors this activity, i.e. large q in Eq (12); conversely silent neurons should predict small values of q . Figure 6c,d shows the distributions $P(q|\sigma)$, assembled by sampling all moments in time when a neuron was active (purple) or silent (yellow). A clear separation between the two distributions indicates that our model really does distinguish network states that drive activity or silence of individual cells. We see that this works for the local subgroup (Fig 6c) but not for the distant subgroup (Fig 6d). It is interesting to note that for the distant subgroup, where prediction quality is much lower, the overlap between the distributions is created by the active neurons' distribution (purple) resembling the silent one (yellow), rather than both changing their shape towards one other. This behavior indicates that for the large selection radius, the model predicts more false negatives, i.e. "misses" predicting the activity of a neuron that was active. Additionally, this suggests false negatives are more difficult to avoid than false positives.

IV. DISCUSSION

Recent technological breakthroughs have made it possible to acquire "big data" on a wide range of living systems, including the brain. The unprecedented scale of these data call for new computational methods of analysis, but it is unclear what we should expect. Should analysis of these larger data sets just test qualitative hypotheses, or are we approaching the point where the data should provide detailed tests of underlying theories? Do simplifying assumptions in our models mean that we should expect only approximate agreement with experiment, or is it possible for simple theories to make quantitatively successful predictions even in such complex systems? Our exploration of maximum entropy models for many examples of $N = 100$ neurons in the same region of the brain provides new perspective on these admittedly ambitious questions.

The models that we have considered are based on a simple theoretical idea, namely that all of the structure that we will see in the patterns of neural activity is encoded in the matrix of pairwise correlations. We can view

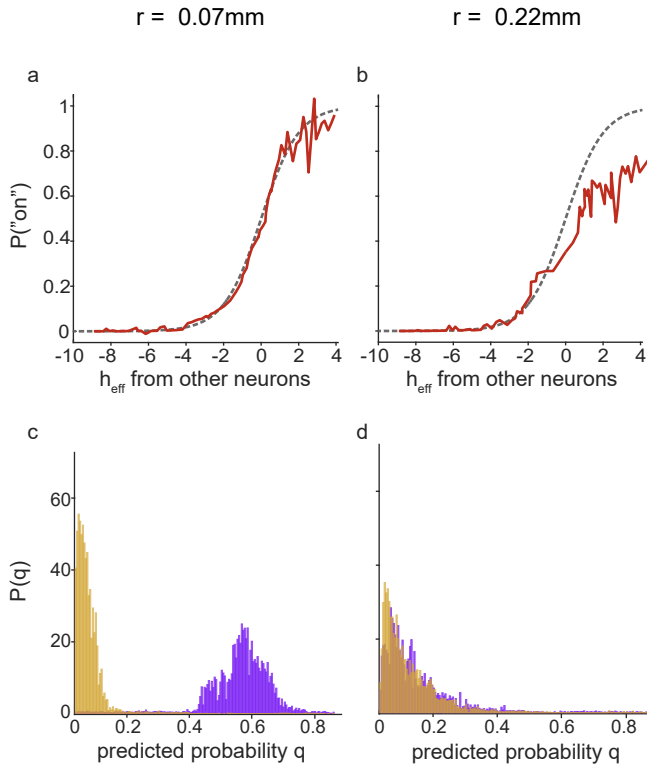


FIG. 6: Population effective field and predicted probability to be active. (a) Probability of neuron to be active based on effective field, as defined in Eq (11) computed for the “local” subgroup. In red, the relationship between the calculated effective field and the probability of a neuron to be active. The dashed line indicates the parameter-free prediction in Eq (11). (b) Same as panel a, computed for the “distant” subgroup. (c) Predicted conditional probability distributions for all neurons to be active/silent for all time points, computed for the “local” subgroup. $P(\sigma_i = 1 | h_{\text{eff}})$: time points where the neuron is active in the data, depicted in purple. $P(\sigma_i = 0 | h_{\text{eff}})$: time points where the neurons are inactive, depicted in yellow. (d) Same as panel c, computed for the “distant” subgroup. The overlap between the two distributions has increased to the point that it is impossible to distinguish the values between the two.

the maximum entropy construction just as a computing engine to decode these predictions. Importantly, with $N \sim 100$ neurons and reasonable recording times, these pairwise correlations can be measured reliably, and so all subsequent predictions are parameter-free. What have we learned from the tests of these predictions in Figs 4, 5, and 6?

The first conclusion is that the parameter-free predictions of simple theories can agree with real biological data in surprising quantitative detail. For local subgroups of neurons, all of the predictions that we test agree with experiment within the errors of our measurement. These tests include detailed wiggles in the distribution of “energy” across all the observed states of the population (Fig 4c), the $\sim 10^5$ individual correlations among triplets of

neurons (Fig 5c), and the dependence of activity in one cell on the state of the whole network (Fig 6a). Although we have focused on one group of $N = 100$ cells, this same level of agreement is found in thirty different local subgroups across three different mice, as will be described in detail in a longer paper.

The second conclusion is that this success is not guaranteed: we can choose a different group of $N = 100$ neurons from the same area of the brain, with very similar patterns of mean activity and pairwise correlations in response to the same behaviors, and the predictions of the simple model fail. These failures range from modest disagreements in the probability that K out of N neurons are active simultaneously (Fig 4b) to missing the bulk of the triplet correlations (Fig 5b), and underestimating the dependence of an individual neuron’s activity on the state of the network (Fig 6b). These results again are consistent: theory disagrees with experiment, with deviations well outside experimental error, for all of the thirty different distant subgroups that we have tested.

A corollary of these two conclusions is that we need to be very careful in saying that we have agreement or disagreement between theory and experiment. If one looks only at what we have described as “failures,” one might be tempted to say that the models in fact capture trends in the data, and that the failure to reach quantitative agreement is the result of over-simplification. In fact this is not the case, since we achieve detailed quantitative agreement using the same theory to describe a different group of cells in the same area under the same conditions.

This leads to a third conclusion, that success or failure of our predictions must reflect properties of the underlying network. In this case, success is found when we describe a densely sampled collection of cells from a contiguous region, and failure is associated with sparse sampling from a larger region. This suggests that effective interactions among neurons are more local, so that in drawing a tight circle around $N = 100$ cells we come closer to capturing a complete network. Completeness is important since even if the real network is perfectly described by a pairwise maximum entropy model, averaging over unobserved neurons generates effective higher-order interactions. If this effect is sufficiently strong, then a pairwise model will fail to describe the subgroup of cells that we observe.

The literature provides conflicting evidence regarding the spatial structure of either connections or correlations in the dorsal hippocampus. While some studies argue that cells in close proximity share spatio-temporal activity characteristics [43, 44], others conclude the opposite [58, 59]. Moreover, theoretical models propose that in order to arbitrarily associate activity patterns in different contexts, and to maximize memory capacity by mapping similar inputs onto very different internal representation, there should be minimal correlation in the synaptic drive to nearby neurons [60–64], although this proposal is inconsistent with the general tendency of neighboring neurons to exhibit correlated activity [65]. Finally, maybe

the most clear cut piece of evidence as to whether proximal cells in the hippocampus are more likely to affect each other is provided by advanced single-cell optical perturbations [45]. These experiments show that manipulating single place-cell activity also affects activity in small groups of other neurons that were simultaneously active around it, strongly indicating a functional role for local interactions in shaping activity patterns and consistent with the pattern of success and failure that we find for our simple models.

Acknowledgments

Work supported in part by the National Science Foundation through the Center for the Physics of Biological

Function (PHY-1734030); by the Simons Collaboration on the Global Brain; by the Howard Hughes Medical Institute; and by the Swartz Foundation. This paper is dedicated to the memory of Cristina Domnisoru, a luminary who inspired so many; a continuing source of brilliance, creativity, and wonder. Cristina burned selflessly and incisively to better the world, and leaves a lasting echo in her wake.

[1] Nicholas A Steinmetz, Christof Koch, Kenneth D Harris, and Matteo Carandini. Challenges and opportunities for large-scale electrophysiology with neuropixels probes. *Curr. Opin. Neurobiol.*, 50:92–100, 2018.

[2] Nicholas A Steinmetz, Cagatay Aydin, Anna Lebedeva, Michael Okun, Marius Pachitariu, Marius Bauza, Maxime Beau, Jai Bhagat, Claudia Böhm, Martijn Broux, et al. Neuropixels 2.0: A miniaturized high-density probe for stable, long-term brain recordings. *Science.*, 372(6539), 2021.

[3] Jason E Chung, Hannah R Joo, Jiang Lan Fan, Daniel F Liu, Alex H Barnett, Supin Chen, Charlotte Geaghan-Breiner, Mattias P Karlsson, Magnus Karlsson, Kye Y Lee, et al. High-density, long-lasting, and multi-region electrophysiological recordings using polymer electrode arrays. *Neuron.*, 101(1):21–31, 2019.

[4] David Tsai, Daniel Sawyer, Adrian Bradd, Rafael Yuste, and Kenneth L Shepard. A very large-scale microelectrode array for cellular-resolution electrophysiology. *Nat. Commun.*, 8(1):1–11, 2017.

[5] Misha B Ahrens, Michael B Orger, Drew N Robson, Jennifer M Li, and Philipp J Keller. Whole-brain functional imaging at cellular resolution using light-sheet microscopy. *Nat. Methods*, 10(5):413–420, 2013.

[6] Nicholas James Sofroniew, Daniel Flickinger, Jonathan King, and Karel Svoboda. A large field of view two-photon mesoscope with subcellular resolution for in vivo imaging. *Elife*, 5:e14472, 2016.

[7] Fritjof Helmchen and Winfried Denk. Deep tissue two-photon microscopy. *Nat. Methods*, 2(12):932–940, 2005.

[8] Lin Tian, Jasper Akerboom, Eric R Schreiter, and Loren L Looger. Neural activity imaging with genetically encoded calcium indicators. *Prog. Brain Res.*, 196:79–94, 2012.

[9] Siegfried Weisenburger, Frank Tejera, Jeffrey Demas, Brandon Chen, Jason Manley, Fraser T Sparks, Francisco Martínez Traub, Tanya Daigle, Hongkui Zeng, Attila Losonczy, et al. Volumetric Ca^{2+} imaging in the mouse brain using hybrid multiplexed sculpted light microscopy. *Cell.*, 177(4):1050–1066, 2019.

[10] Jeffrey D Orth, Tom M Conrad, Jessica Na, Joshua A Lerman, Hojung Nam, Adam M Feist, and Bernhard Ø Palsson. A comprehensive genome-scale reconstruction of *Escherichia coli* metabolism. *Mol. Syst. Biol.*, 7(1):535, 2011.

[11] Yann LeCun, Yoshua Bengio, and Geoffrey Hinton. Deep learning. *Nature.*, 521(7553):436–444, 2015.

[12] Alex Krizhevsky, Ilya Sutskever, and Geoffrey E Hinton. Imagenet classification with deep convolutional neural networks. *NeurIPS.*, 25:1097–1105, 2012.

[13] Karen Simonyan and Andrew Zisserman. Very deep convolutional networks for large-scale image recognition. *arXiv preprint arXiv:1409.1556*, 2014.

[14] Ryan J Low, Sam Lewallen, Dmitriy Aronov, Rhino Neversons, and David W Tank. Probing variability in a cognitive map using manifold inference from neural dynamics. *BioRxiv*, page 418939, 2018.

[15] Juan A Gallego, Matthew G Perich, Lee E Miller, and Sara A Solla. Neural manifolds for the control of movement. *Neuron*, 94(5):978–984, 2017.

[16] Edward H Nieh, Manuel Schottendorf, Nicolas W Freeman, Ryan J Low, Sam Lewallen, Sue Ann Koay, Lucas Pinto, Jeffrey L Gauthier, Carlos D Brody, and David W Tank. Geometry of abstract learned knowledge in the hippocampus. *Nature*, 595:80–84, 2021.

[17] Saurabh Vyas, Matthew D Golub, David Sussillo, and Krishna V Shenoy. Computation through neural population dynamics. *Annu. Rev. Neurosci.*, 43:249–275, 2020.

[18] James Sethna. *Statistical Mechanics: Entropy, Order Parameters, and Complexity*, volume 14. Oxford University Press, USA, 2021.

[19] Edwin T Jaynes. Information theory and statistical mechanics. *Phys. Rev.*, 106(4):620, 1957.

[20] Edwin T Jaynes. On the rationale of maximum-entropy methods. *Proc. IEEE*, 70(9):939–952, 1982.

[21] Gaia Tavoni, Ulisse Ferrari, Francesco P Battaglia, Simona Cocco, and Rémi Monasson. Functional coupling networks inferred from prefrontal cortex activity show experience-related effective plasticity. *Netw. Neurosci.*, 1(3):275–301, 2017.

[22] Ifiye E Ohiorhenuan, Ferenc Mechler, Keith P Purpura, Anita M Schmid, Qin Hu, and Jonathan D Victor. Sparse coding and high-order correlations in fine-scale cortical networks. *Nature*, 466(7306):617–621, 2010.

[23] Gasper Tkacik, Elad Schneidman, Michael J Berry II, and William Bialek. Ising models for networks of real neurons. *arXiv preprint q-bio/0611072*, 2006.

[24] Gasper Tkacik, Elad Schneidman, Michael J Berry II, and William Bialek. Spin glass models for a network of real neurons. *arXiv preprint arXiv:0912.5409*, 2009.

[25] Gašper Tkačik, Olivier Marre, Thierry Mora, Dario Amodei, Michael J Berry II, and William Bialek. The simplest maximum entropy model for collective behavior in a neural network. *J. Stat. Mech. Theory Exp.*, 2013(03):P03011, 2013.

[26] Elad Schneidman, Michael J Berry, Ronen Segev, and William Bialek. Weak pairwise correlations imply strongly correlated network states in a neural population. *Nature.*, 440(7087):1007–1012, 2006.

[27] Einat Granot-Atedgi, Gašper Tkačik, Ronen Segev, and Elad Schneidman. Stimulus-dependent maximum entropy models of neural population codes. *PLoS Comput. Biol.*, 9(3):e1002922, 2013.

[28] Alan Lapedes, Bertrand Giraud, and Christopher Jarzynski. Using sequence alignments to predict protein structure and stability with high accuracy. *arXiv preprint arXiv:1207.2484*, 2012.

[29] Anne-Florence Bitbol, Robert S Dwyer, Lucy J Colwell, and Ned S Wingreen. Inferring interaction partners from protein sequences. *Proc. Natl. Acad. Sci. (USA)*, 113(43):12180–12185, 2016.

[30] Debora S Marks, Lucy J Colwell, Robert Sheridan, Thomas A Hopf, Andrea Pagnani, Riccardo Zecchina, and Chris Sander. Protein 3d structure computed from evolutionary sequence variation. *PLoS One*, 6(12):e28766, 2011.

[31] William P Russ, Matteo Figliuzzi, Christian Stocker, Pierre Barrat-Charlaix, Michael Socolich, Peter Kast, Donald Hilvert, Remi Monasson, Simona Cocco, Martin Weigt, et al. An evolution-based model for designing chorismate mutase enzymes. *Science*, 369(6502):440–445, 2020.

[32] Lorenzo Asti, Guido Uguzzoni, Paolo Marcattili, and Andrea Pagnani. Maximum-entropy models of sequenced immune repertoires predict antigen-antibody affinity. *PLoS Comput. Biol.*, 12(4):e1004870, 2016.

[33] Thierry Mora, Aleksandra M Walczak, William Bialek, and Curtis G Callan. Maximum entropy models for antibody diversity. *Proc. Natl. Acad. Sci. (USA)*, 107(12):5405–5410, 2010.

[34] William Bialek, Andrea Cavagna, Irene Giardina, Thierry Mora, Edmondo Silvestri, Massimiliano Viale, and Aleksandra M Walczak. Statistical mechanics for natural flocks of birds. *Proc. Natl. Acad. Sci. (USA)*, 109(13):4786–4791, 2012.

[35] William Bialek, Andrea Cavagna, Irene Giardina, Thierry Mora, Oliver Pohl, Edmondo Silvestri, Massimiliano Viale, and Aleksandra M Walczak. Social interactions dominate speed control in poising natural flocks near criticality. *Proc. Natl. Acad. Sci. (USA)*, 111(20):7212–7217, 2014.

[36] Jakob H Macke, Iain Murray, and Peter E Latham. How biased are maximum entropy models? In *NeurIPS*, pages 2034–2042, 2012.

[37] Yasser Roudi, Sheila Nirenberg, and Peter E Latham. Pairwise maximum entropy models for studying large biological systems: when they can work and when they can't. *PLoS Comput. Biol.*, 5(5):e1000380, 2009.

[38] Francisco Barahona. On the computational complexity of ising spin glass models. *J. Phys. A: Math. Gen.*, 15(10):3241, 1982.

[39] Brad A Radvansky and Daniel A Dombeck. An olfactory virtual reality system for mice. *Nat. Commun.*, 9(1):1–14, 2018.

[40] Weijian Zong, Runlong Wu, Mingli Li, Yanhui Hu, Yijun Li, Jinghang Li, Hao Rong, Haitao Wu, Yangyang Xu, Yang Lu, et al. Fast high-resolution miniature two-photon microscopy for brain imaging in freely behaving mice. *Nat. Methods*, 14(7):713–719, 2017.

[41] Jeffrey L Gauthier and David W Tank. A dedicated population for reward coding in the hippocampus. *Neuron*, 99(1):179–193, 2018.

[42] Leenoy Meshulam, Jeffrey L Gauthier, Carlos D Brody, David W Tank, and William Bialek. Collective behavior of place and non-place neurons in the hippocampal network. *Neuron*, 96(5):1178–1191, 2017.

[43] SI Wiener, CA Paul, and H Eichenbaum. Spatial and behavioral correlates of hippocampal neuronal activity. *J. Neurosci.*, 9(8):2737–2763, 1989.

[44] Robert E Hampson, John D Simeral, and Sam A Deadwyler. Distribution of spatial and nonspatial information in dorsal hippocampus. *Nature.*, 402(6762):610–614, 1999.

[45] John Peter Rickgauer, Karl Deisseroth, and David W Tank. Simultaneous cellular-resolution optical perturbation and imaging of place cell firing fields. *Nat. Neurosci.*, 17(12):1816–1824, 2014.

[46] Jeff L Gauthier, Sue Ann Koay, Edward H Nieh, David W Tank, Jonathan W Pillow, and Adam S Charles. Detecting and correcting false transients in calcium imaging. *bioRxiv*, page 473470, 2018.

[47] John O’Keefe and Lynn Nadel. *The Hippocampus as a Cognitive Map*. Oxford university press, 1978.

[48] John O’Keefe. A review of the hippocampal place cells. *Prog. Neurobiol.*, 13(4):419–439, 1979.

[49] Daniel A Dombeck, Christopher D Harvey, Lin Tian, Loren L Looger, and David W Tank. Functional imaging of hippocampal place cells at cellular resolution during virtual navigation. *Nat. Neurosci.*, 13(11):1433–1440, 2010.

[50] Eftychios A Pnevmatikakis and Liam Paninski. Sparse nonnegative deconvolution for compressive calcium imaging: algorithms and phase transitions. In *NeurIPS*, pages 1250–1258. Citeseer, 2013.

[51] Eftychios A Pnevmatikakis, Daniel Soudry, Yuanjun Gao, Timothy A Machado, Josh Merel, David Pfau, Thomas Reardon, Yu Mu, Clay Lacefield, Weijian Yang, et al. Simultaneous denoising, deconvolution, and demixing of calcium imaging data. *Neuron*, 89(2):285–299, 2016.

[52] Sean W Jewell, Toby Dylan Hocking, Paul Fearnhead, and Daniela M Witten. Fast nonconvex deconvolution of calcium imaging data. *Biostatistics*, 21(4):709–726, 2020.

[53] Claude Elwood Shannon. A mathematical theory of communication. *The Bell system technical journal*, 27(3):379–423, 1948.

[54] Marc Mezard, Giorgio Parisi, Miguel Angel Virasoro, and David J Thouless. Spin glass theory and beyond. *Phys. Today*, 41(12):109, 1988.

[55] Elad Ganmor, Ronen Segev, and Elad Schneidman. Sparse low-order interaction network underlies a highly

correlated and learnable neural population code. *Proc. Natl. Acad. Sci. (USA)*, 108(23):9679–9684, 2011.

[56] Gašper Tkačik, Olivier Marre, Dario Amodei, Elad Schneidman, William Bialek, and Michael J Berry. Searching for collective behavior in a large network of sensory neurons. *PLoS Comput. Biol.*, 10(1):e1003408, 2014.

[57] Josiah Willard Gibbs. *Elementary principles in statistical mechanics: developed with especial reference to the rational foundations of thermodynamics*. C. Scribner's sons, 1902.

[58] A David Redish, Francesco P Battaglia, Monica K Chawla, Arne D Ekstrom, Jason L Gerrard, Peter Lipa, Ephron S Rosenzweig, Paul F Worley, John F Guzowski, Bruce L McNaughton, et al. Independence of firing correlates of anatomically proximate hippocampal pyramidal cells. *J. Neurosci.*, 21(5):RC134–RC134, 2001.

[59] Kenneth D Harris, Jozsef Csicsvari, Hajime Hirase, George Dragoi, and György Buzsáki. Organization of cell assemblies in the hippocampus. *Nature.*, 424(6948):552–556, 2003.

[60] David Marr and W Thomas Thach. A theory of cerebellar cortex. In *From the Retina to the Neocortex*, pages 11–50. Springer, 1991.

[61] NJ Cohen and H Eichenbaum. *Memory, Amnesia, and the Hippocampal System*. The MIT Press, Cambridge, MA, 1993.

[62] James L McClelland, Bruce L McNaughton, and Randall C O'Reilly. Why there are complementary learning systems in the hippocampus and neocortex: insights from the successes and failures of connectionist models of learning and memory. *Psychol. review*, 102(3):419, 1995.

[63] Bruce L McNaughton, Carol A Barnes, J Meltzer, and RJ Sutherland. Hippocampal granule cells are necessary for normal spatial learning but not for spatially-selective pyramidal cell discharge. *Exp. Brain Res.*, 76(3):485–496, 1989.

[64] A David Redish et al. *Beyond the Cognitive Map: From Place Cells to Episodic Memory*. MIT press, 1999.

[65] Taylor W. Schmitz and John Duncan. Normalization and the cholinergic microcircuit: A unified basis for attention. *Trends Cogn. Sci.*, 22(5):422–437, 2018.